Evidence for Conformational Dynamics and Molecular Aggregation in Cytochrome P450 102 (BM-3)†

Shaun D. Black* and Suzanne T. Martin

Department of Biochemistry, University of Texas Health Center at Tyler, Tyler, Texas 75710-2003

Received May 16, 1994; Revised Manuscript Received August 1, 1994®

ABSTRACT: The native molecular weight of affinity-purified cytochrome P450 102 from barbiturate-induced *Bacillus megaterium* has been studied by sedimentation methods and HPLC size-exclusion chromatography. Sedimentation velocity experiments yielded an $s^0_{20,w}$ = 9.244 S for the holocytochrome, but the diffusion coefficient was unexpectedly large and varied widely with centrifugal field, ionic strength, and protein concentration. Addition of 50 mM DL-dithiothreitol (DTT) caused a small decrease in the value of $s^0_{20,w}$, but D_{20} still did not behave as expected. The sedimentation coefficients were consistent with a molecular weight of about 200 000, and the diffusion coefficients indicated molecular aggregation. Sedimentation equilibrium analyses suggested that the native enzyme was a mixture of monomer, dimer, trimer, and tetramer. However, after incubation of P450 102 with DTT, sedimentation equilibrium demonstrated that the enzyme was dimeric (molecular weight 236 000). HPLC size-exclusion chromatography of the cytochrome showed the presence of four peaks, which corresponded to 1.45-mer, 2.06-mer, 3.02-mer, and a higher molecular weight fraction; aggregated forms accounted for about 52% of the P450 102. Incubation of the enzyme with DTT caused a shift toward the 1.45-mer, but dimer, trimer, and the high molecular weight peak still persisted; the shift was not attributable to disulfide bond reduction. The 1.45-mer was determined to be a monomeric species of significantly asymmetric geometry. Together, the results indicated that cytochrome P450 exists with monomer, dimer, trimer, etc. in equilibrium, contrary to the expectation that this soluble P450 would be monomeric. Additional size-exclusion HPLC experiments confirmed the existence of equilibria among molecular aggregates, identified the reductase domain as the site of aggregation, and showed that the P450 102 monomer peak could elute with a variety of apparent aggregation states, between 1.13 and 1.45. These latter data showed the presence of conformational dynamics, at least in the monomer.

The cytochrome P450[1] superfamily presently numbers more than 300 structurally-characterized enzymes (Nelson et al., 1993). The eukaryotic P450s are generally membrane-bound and are localized principally in the endoplasmic reticulum and mitochondria (Black, 1992; Black & Coon, 1987; Schenkman & Greim, 1993; Waterman & Johnson, 1991). In contrast, the prokaryotic P450s are all soluble, yet still resemble either the microsomal or the mitochondrial monooxygenase systems (Sariaslani, 1991).

Cytochrome P450 102 (P450 BM-3) is presently the only prokaryotic P450 known to resemble the mammalian microsomal P450 monooxygenases. The enzyme was first purified to homogeneity from the bacterium *Bacillus megaterium* by Narhi and Fulco (1986) and has been shown to bear strong sequence homology to the fatty acid ω-hydroxylases. This soluble enzyme is unusual in that it contains both a flavoprotein reductase and a P450 component in a single polypeptide chain of 1048 residues (Miles et al., 1992; Narhi & Fulco, 1987; Ruettinger et al., 1989), whereas the mammalian microsomal P450s retain these two functional elements as two separate proteins. The three-dimensional structure of the P450 102 heme domain has been described (Li et al., 1991; Ravichandran et al., 1993). The flavin domain has been shown to be composed of two further domains: one which binds FMN and another which binds FAD/NADP(H) (Oster et al., 1991). In the presence of NADPH and molecular oxygen, the holoenzyme supports hydroxylation of long-chain fatty acids with rapid rates of catalysis (Black et al., 1994; Boddupalli et al., 1990, 1992; Narhi & Fulco, 1986). However, like its mammalian counterparts, P450 102 also exhibits broad substrate specificity (Black et al., 1994). P450 102 is inducible by a variety of compounds, including barbiturates (Kim & Fulco, 1983) and acyl ureas (Ruettinger et al., 1984), thus providing yet another mode of similarity to the mammalian P450 monooxygenases (Conney, 1967).

Our laboratory has been interested in structure–function relationships in cytochrome P450 102 as a means to understand the mammalian monooxygenase system. In the present study, hydrodynamic data are given which show that the structure of the enzyme in aqueous solution is complex, representing a distribution of aggregated forms; this is in contrast to what was anticipated from the soluble character of the enzyme. Furthermore, evidence has been gathered to show that the monomer unit of P450 102 exhibits significant conformational dynamics. A preliminary report of these findings has been presented (Black & Martin, 1994).

EXPERIMENTAL PROCEDURES

Purification of Cytochrome P450 102 from Bacillus megaterium. Growth, induction with 5 mM sodium pento-

† This research was supported by Grant GM38261 from the National Institutes of Health.

* Author to whom correspondence should be addressed at the Department of Biochemistry, University of Texas Health Center at Tyler, P.O. Box 2003, Tyler, TX 75710. Phone: (903) 877-2806. FAX: (903) 877-7558. E-Mail: shaun@jason.uthct.edu.

® Abstract published in *Advance ACS Abstracts,* September 1, 1994.

[1] Abbreviations: cytochrome P450 102 (BM-3), the major barbiturate-inducible isoform in the bacterium *Bacillus megaterium* in accordance with proposed systematic nomenclature (Nelson et al., 1993); DTT, DL-1,4-dithiothreitol; HPLC, high-performance liquid chromatography; SDS–PAGE, sodium dodecyl sulfate–polyacrylamide gel electrophoresis.

0006-2960/94/0433-12056$04.50/0

barbital, harvest, and breakage of *Bacillus megaterium* ATCC 14581 were performed as described (Black et al., 1994). The cytochrome was purified to homogeneity by affinity chromatography on adenosine 2′,5′-diphosphate–agarose, as reported (Black et al., 1994). Protein concentration was estimated with the bicinchoninic acid (BCA) assay (Smith et al., 1985) with crystalline bovine serum albumin as standard. SDS–PAGE was carried out after the method of Laemmli (1970), as modified (Haugen & Coon, 1976).

Determination of Holoenzyme Monomer Molecular Weight and Protein Partial Specific Volume. The holoenzyme monomeric molecular weight of cytochrome P450 102 was computed from the published sequence (Ruettinger et al., 1989) with omission of the initiator methionine (1048 total residues, 117 517 g/mol), and inclusion of cofactors FMN (MW 478.3), FAD (MW 807.6), and heme (MW 616.5) to yield a value of 119 419 g/mol. The partial specific volume, $\bar{\nu}$, was calculated (Creighton, 1984) from the amino acid composition of P450 102. Because $\bar{\nu}$ values were not available for FAD and heme, we assumed that the partial specific volumes of the cofactors approximated that of an average amino acid residue. The resulting value, $\bar{\nu} = 0.721$ cm^3/g, was reasonable relative to other similar proteins.

Measurement of Solvent Density and Viscosity. Density, ρ, was measured by weighing precise aliquots of pure water or buffer solution at 20.0 °C. Average values (4–6 replicates per solution) obtained were as follows: water, $\rho = 0.9943 \pm 0.0009$ g/cm^3 (literature value, 0.9982 g/cm^3); 50 mM, 0.1 M, 0.3 M, or 0.5 M phosphate buffers, pH 7.4, $\rho = 1.0030 \pm 0.0019$, 1.0068 ± 0.0007, 1.0406 ± 0.00165, and 1.0667 ± 0.0008 g/cm^3, respectively. Viscosities were measured at (21.8–22.2) ± 0.1 °C with a laboratory-constructed capillary viscometer having a dispensing volume of 10.0 mL; measurements of outflow time were carried out in 15–16 replicates per solution. Average time values were the following: water, 18.193 ± 0.059 s; 50 mM, 0.1 M, 0.3 M, or 0.5 M phosphate buffers, pH 7.4, 18.213 ± 0.064, 18.231 ± 0.087, 18.540 ± 0.051, and 18.731 ± 0.095 s, respectively. Using a literature value of $\eta_{o(\text{pure water},20\,^\circ\text{C})} = 1.004$ cP (Weast, 1988) and densities as measured above, viscosities at 20 °C were calculated relative to the measured outflow time for pure water, for 50 mM, 0.1 M, 0.3 M, or 0.5 M phosphate buffers, pH 7.4, as 1.0139, 1.0226, 1.0708, and 1.1089 cP, respectively. The equation employed was $\eta = \eta_o[(t/t_o)(\rho/\rho_o)]$, where η and η_o are the viscosities of buffer and water, respectively, t and t_o are the outflow times of buffer and water, respectively, and ρ and ρ_o are the densities of buffer and water, respectively. The final η for each buffer is given for 20.0 °C; small temperature differences in some of the values used caused only insignificant changes in the resulting viscosities.

Sedimentation Studies. Ultracentrifugation was performed with a Beckman Optima XL-A analytical ultracentrifuge with dual-beam detection at 278 or 418 nm, and with an An-60Ti rotor having sectored cells composed of quartz and carbon-impregnated Epon; the cell path length was 1.2065 cm, and the extinction coefficient for cytochrome P450 102 at 278 nm was determined to be 1.448 ± 0.136 (mg/mL)$^{-1}$(cm)$^{-1}$ (n = 10). Sedimentation analyses were carried out at 20.0 °C in 50 mM, 0.1 M, 0.3 M, or 0.5 M potassium phosphate buffer, pH 7.4, with or without 50 mM DTT present. Samples containing DTT were incubated with the reagent for a minimum of 24 h at 4 °C before analysis. Data acquisition and computational analyses were with Beckman Instruments software XLA, XLAVU, XLAVEL, VelGamma, XLAEQ, Origin-Single, and Origin-Multi. Friction factor and hydration calculations were performed according to Laue and Rhodes (1990) and Waxman et al. (1993); protein hydration was assumed to be 0.28 g of water/g of protein.

In sedimentation velocity studies, sedimentation coefficients (s_{20}) were computed from a series of 15–20 absorbance *vs* radial position scans taken at various times during any given experiment; each scan at a given time point was the average of 4 replicate determinations. Sample volumes were 400 μL, and reference cells contained 425 μL of the same buffer. Three different protein concentrations between 0.1 and 0.7 mg/mL were studied for each concentration of phosphate buffer, and centrifugal fields of 7400*g*, 29600*g*, 66700*g*, and 90700g (at $r_{\text{average}} = 6.625$ cm) were examined with 0.1 M potassium phosphate, pH 7.4. Goodness-of-fit between absorbance scans and simulated data was calculated, and scans which yielded minimum error in a χ^2 analysis were accepted; fitting was via a Simplex algorithm. Resulting s_{20} values were extrapolated to infinite protein dilution to obtain s^0_{20}. Each s^0_{20} value was corrected for buffer density and viscosity with the equation $s^0_{20,w} = s^0_{20}[(1 - \rho_{20,w})/(1 - \bar{\nu}\rho)](\eta/\eta_o)$, where $\rho_{20,w}$ is the density of water at 20 °C, ρ is the density of the buffer solution, η is the viscosity of the buffer solution, and η_o is the viscosity of water at 20 °C. The four final $s^0_{20,w}$ values were extrapolated to infinite buffer dilution to obtain the overall sedimentation coefficient for cytochrome P450 102. To assess the potential accuracy and precision of our determinations, a control sedimentation velocity experiment was conducted with bovine serum albumin, yielding an $s_{20} = 4.476$ S, a value identical to literature determinations. Apparent diffusion coefficients, D_{20}, were calculated with a second moment analysis (Muramatsu & Minton, 1988). Sedimentation and diffusion coefficients for standard globular proteins were obtained from the literature (Smith, 1970; Creighton, 1984; Kumosinski & Pessen, 1985).

Sedimentation equilibrium studies were carried out with the same instrument and in the same cells as in the above sedimentation velocity experiments, but sample volumes were 100 μL and reference sectors contained 115 μL of the respective buffer. P450 102 was present in concentrations of 0.18–0.26 mg/mL in 0.1 M potassium phosphate buffer, pH 7.4, with or without 50 mM DTT. Centrifugal fields of 2817*g* and 5009*g* were studied. When samples presumably reached equilibrium, 4–5 scans separated by 1 h each were performed. Equilibrium was assessed to be present in all scans that showed no further change in radial absorbance.

High-Performance Liquid Chromatography. HPLC size-exclusion experiments were performed with a TosoHaas TSK-3000SW$_{XL}$ stationary phase (5 μm particles, 250 Å pore, 7.8 × 300 mm), and a mobile phase of 0.1 M potassium phosphate 0.1 M potassium chloride, pH 7.4. Separations were carried out isocratically at a flow rate of 1.0 mL/min and at 25 °C. The mobile phase was of a higher ionic strength than that used in the sedimentation experiments due to the observation that when analyses were carried out in 0.1 M potassium phosphate, pH 7.4, or 0.1 M Tris, pH 7.4, the apparent molecular weights of all species "increased", and many standards began to deviate from linearity, likely due to adsorptive effects. Standards used for molecular weight calibration were blue dextran (M_r 2 000 000), mouse immunoglobulin M (M_r 890 000), bovine thyroglobulin (M_r 670 000), *Escherichia coli* β-galactosidase (tetramer M_r 540 000), rabbit aldolase (tetramer M_r 160 000), bovine immunoglobulin G (M_r 158 000), bovine alkaline phosphatase (dimer M_r 140 000), jack bean concanavalin A (tetramer M_r 102 400), bovine serum albumin (M_r 68 000), ovalbumin (M_r

43 500), bovine chymotrypsinogen (M_r 25 700), horse myoglobin (M_r 17 000), horse cytochrome *c* (M_r 12 300), and vitamin B_{12} (M_r 1350). The presence of monomer/dimer equilibria in concanavalin A and bovine albumin, and dimer/tetramer equilibria in β-galactosidase and aldolase, provided additional data for use in molecular weight calibration. Each standard was analyzed at least in triplicate. The void volume of the column was 5.29 mL, and the included volume was 11.36 mL.

RESULTS

Sedimentation Velocity Studies on Cytochrome P450 102. Sedimentation analyses were carried out with three concentrations of P450 102 at each of four phosphate buffer concentrations. In addition, four centrifugal fields were studied at fixed protein concentration and buffer composition. Visual inspection of the radial scans suggested a smooth, single-phase transition during sedimentation. Plots of dAbs/d*r* *vs* *r* showed a rather symmetrical Gaussian character, though peaks were somewhat broader than expected. With regard to the sedimentation coefficient, data quality was excellent with $\ln(r_{inflection} - r_{meniscus})$ *vs* $\omega^2 t$ plots exhibiting linearity with correlation coefficients ≥0.999. Sedimentation coefficients (s^0_{20}) showed essentially no dependence on protein concentration, as the slope of $1/s$ *vs* [P450 102] plots was essentially zero; thus, s^0_{20} approximated s_{20}. Similarly, the ionic strength of the medium had essentially no effect on the sedimentation coefficient, but a mild dependence of the centrifugal field was observed (see below). We performed some analyses at both 278 and 418 nm to examine, respectively, the sedimentation of the polypeptide and cofactors, and found that calculated sedimentation coefficients were essentially identical. Thus, cofactors were not dissociating from the enzyme during sedimentation. The overall sedimentation coefficient of cytochrome P450 was arrived at after correction for protein concentration, buffer density and viscosity, and ionic strength of the medium; $s^0_{20,w} = 9.244 \times 10^{-13}$ s (9.244 S).

The apparent diffusion coefficient, D_{20}, measured for cytochrome P450 102 at 66700*g* in 0.1 M potassium phosphate buffer, pH 7.4, was 7.95×10^{-7} cm²/s. This value was larger than that expected by comparison to other hydrodynamically characterized soluble, globular proteins. Such a comparison is shown in Figure 1, where the point for P450 102 is seen to lie significantly off the fit curve. Of note in this connection is the observation that a few other proteins also exhibit anomalous behavior on the *s* *vs* *D* plot, and this behavior appears to run effectively parallel to the fit curve for globular proteins. The measured D_{20} values varied widely as a function of buffer concentration, increased radial distance during sedimentation, and centrifugal field. Over all experiments, the values ranged from 3.10×10^{-7} to 18.96×10^{-7} cm²/s. The effect of centrifugal field on both s_{20} and D_{20} is studied in Figure 2. As noted above, s^0_{20} showed only mild dependence on the centrifugal field. In contrast, D_{20} showed an apparently linear ($r = 0.997$) and significant dependence on the applied field (slope = $0.0853D/g$). The effect of ionic strength on D_{20} (data not shown) was similarly marked, showing increased values of the apparent diffusion coefficient at increased ionic strength. The effect of protein concentration was less dramatic, but the apparent D_{20} showed a tendency to increase with increased protein concentration (data not shown).

In the presence of 50 mM DTT, sedimentation velocity analyses yielded $s^0_{20,w} = (8.507 \pm 0.333) \times 10^{-13}$ s ($n = 2$), a value somewhat smaller than that obtained under similar

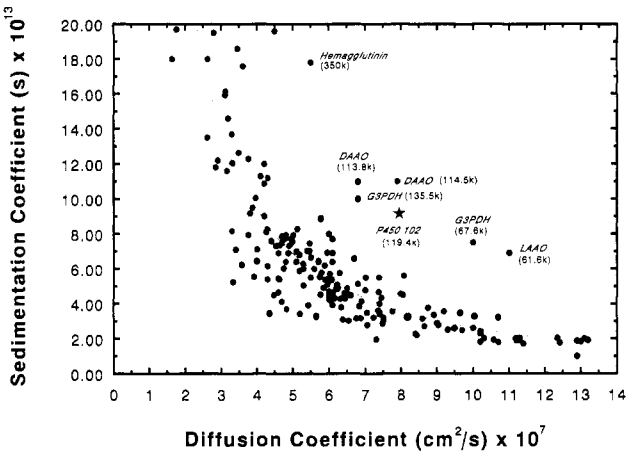

FIGURE 1: Comparison of sedimentation and diffusion coefficients for cytochrome P450 102 and 186 soluble, globular proteins. Values of *s* and *D* for the globular proteins (●) were taken from the literature, as indicated under Experimental Procedures. Curve fitting of these data was via the equation $D = 64.427s^{-1.390}$. The sedimentation coefficient of P450 102 is the $s^0_{20,w}$, and the D_{20} was determined at 66700*g* in 0.1 M potassium phosphate buffer, pH 7.4; these data are indicated with a star (★). Proteins which lie well off the fit line are indicated, with their molecular weights, by the following abbreviations: *Hemagglutinin* (cold human viral hemagglutinin), *DAAO* (Michaelis complexes of porcine D-amino acid oxidases), *G3PDH* (bovine and rabbit D-glyceraldehyde-3-phosphate dehydrogenases), and *LAAO* (moccasin snake L-amino acid oxidase).

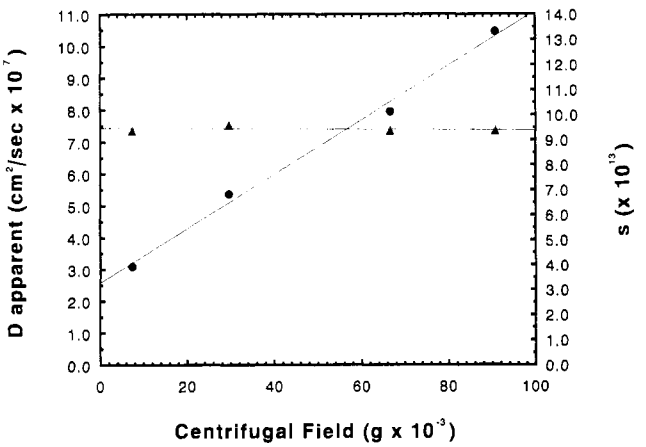

FIGURE 2: Effect of centrifugal field on sedimentation and diffusion coefficients of cytochrome P450 102. Sedimentation velocity analyses were carried out at 20.0 °C, with 0.35 mg/mL protein in 0.1 M potassium phosphate buffer, pH 7.4, under the indicated centrifugal fields. Values of the sedimentation coefficient (▲) and diffusion coefficient (●) are given as s_{20} and D_{20}, respectively.

conditions but in the absence of DTT. D_{20} apparent in the presence of DTT was found to be 5.816×10^{-7} cm²/s, also smaller than the average value seen in the absence of DTT. With reference to Figure 1, the point for $s^0_{20,w}$ and D_{20} in the presence of DTT was still deviant from the ideal curve, though not nearly so much as was seen in the absence of the reagent.

Sedimentation Equilibrium Studies. Sedimentation equilibrium analysis of cytochrome P450 102 in the absence of DTT is shown in Figure 3A. Curve fitting showed that the results could not be fit to any single molecular weight species. However, excellent fits resulted when data were analyzed with a model in which a mixture of monomer, dimer, trimer, and tetramer were in equilibrium. The inset values represent the monomer/dimer, dimer/trimer, and trimer/tetramer association constants that resulted when the fitting routine converged to a minimum χ^2 error (after 168 iterations); residuals appeared to be randomly distributed. K_{a2} and K_{a3} were similar

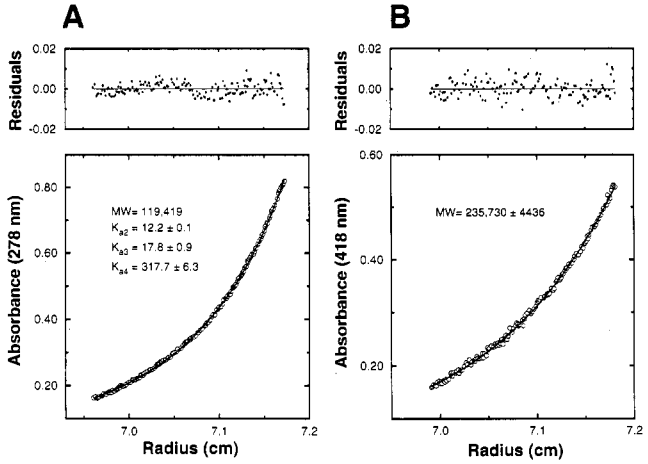

FIGURE 3: Sedimentation equilibrium analyses of cytochrome P450 102 in the absence (A) or presence (B) of 50 mM DTT. Analyses were carried out at 20.0 °C in 0.1 M potassium phosphate buffer, pH 7.4. The lower panel of each portion of the figure represents cell absorbance *vs* radial distance when the solutions had reached equilibrium (O) (15 h at 2817*g*). The curves resulted from iterative mathematical fitting of the data until a χ^2 error function was minimized. The upper panel of each portion of the figure shows residuals between the experimental data and final fit curve. Data obtained in the absence of DTT (panel A) were fit to a model in which monomer, dimer, trimer, and tetramer were in equilibrium; the inset association constants were those obtained for each equilibrium after the completion of curve fitting. The data collected in the presence of DTT (panel B) fit a single molecular species, the molecular weight of which is shown in the inset.

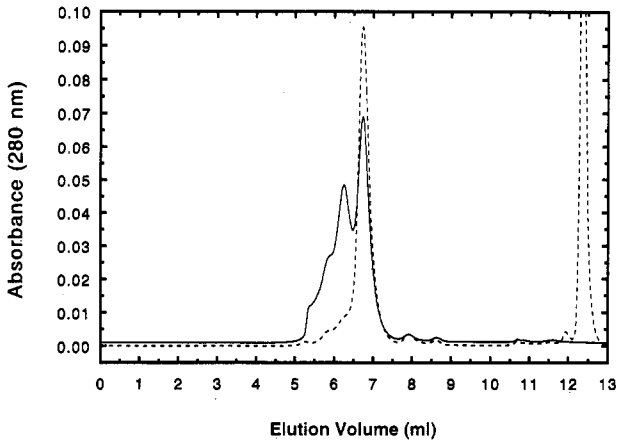

FIGURE 4: Size-exclusion HPLC analysis of cytochrome P450 102 in the absence (—) or presence (- - -) of 50 mM DTT. Analyses were carried out at ambient temperature and with a flow rate of 1.0 mL/min in 0.1 M potassium phosphate/0.1 M potassium chloride, pH 7.4; other experimental details are as described under Experimental Procedures. Oxidized DTT eluted in the vicinity of 12.4 min.

in value, and favored formation of dimer and trimer, respectively. K_{a4} was about 30 times greater, indicating a strong tendency to form tetramer in the linked equilibria. In sharp contrast, analysis of P450 102 in the presence of 50 mM DTT showed linear ln ΔA *vs* r^2 plots, and fits to a single molecular weight form converged quickly with low χ^2 deviance, as shown in Figure 3B. As in the previous fit, the residuals appeared to be randomly distributed. The computed molecular weight was 236 000 ± 4400, a value only 1.9% deviant and statistically indistinguishable from the true holoenzyme dimer molecular weight (238 838). This result indicated that P450 102 was present as a 2.01-mer during sedimentation equilibrium analysis in the presence of DTT.

HPLC Size-Exclusion Analyses. When cytochrome P450 102 was submitted to HPLC gel filtration, as shown in Figure 4, the protein was found to elute as four peaks, at ~5.3, ~5.8, ~6.2, and ~6.7 mL; the lattermost fraction represented the greatest quantity. With reference to the calibration standards analyzed, these four peaks corresponded to M_r 763 800 (partition constant, K_d= 0.017; 6.4-mer; 3.3% of total area), M_r 360 600 (K_d = 0.105; 3.02-mer; 17.8% of total area), M_r 245 500 (K_d= 0.163; 2.06-mer; 30.4% of total area), and M_r 173 400 (K_d = 0.237; 1.45-mer; 47.5% of total area), respectively. No peak corresponded to true monomer. However, when P450 102 was analyzed after incubation with 50 mM DTT, 94% of the enzyme appeared as the 1.5-mer species, but dimer, trimer, and the high molecular weight peak still persisted (6% of total). This observation held true even after 400 h of preincubation with 50 mM DTT at 4 °C before HPLC analysis. The interaction with DTT was at least biphasic, with a $t_{1/2}$ of ~3.6 h for the initial effect and a $t_{1/2}$ of about 19 h for later changes; the reaction was essentially complete after 62 h of preincubation at 4 °C. During the reaction, the trimer species disappeared rapidly, but dimer was much more slowly converted to 1.5-mer; the high molecular weight peak was relatively resistant to disaggregation. We utilized 50 mM DTT because lower concentrations had significantly longer reaction half-times which proved to be experimentally impractical.

We also studied the effect of sodium dithionite and *n*-octyl β-D-glucopyranoside on P450 102 (data not shown). In the case of sodium dithionite, we found that a maximum of 88% 1.5-mer could be produced, but at a slower rate than with 50 mM DTT. In contrast, rather than causing disaggregation, the detergent *n*-octyl β-D-glucopyranoside caused a small increase in the aggregation state of P450 102.

To study further the mechanism of protein–protein association for P450 102, we analyzed domains of the enzyme as well as other related proteins and fragments. The P450 102 heme domain (residues 1–470) chromatographed as a single, monomeric species (aggregation state 0.98-mer). In contrast, the P450 102 FAD/NADP$^+$ domain (residues 646–1048, unpublished results) eluted as multiple peaks in HPLC size-exclusion analyses. The aggregation states present (and percent of total protein) were 1.29-mer (62.6%), 2.34-mer (26.9%), 3.52-mer (6.8%), and 4.86-mer (3.6%). This behavior was similar to that seen with the intact P450 102. The P450 102 complete flavin domain (FMN/FAD/NADP$^+$ domain, residues 472–1048) ran as an M_r 63 900, 1.27-mer and other aggregated forms. The 1.27-mer and other molecular aggregates of this fragment eluted with aggregation states similar to those seen with the FAD/NADP$^+$ domain. Trypsin-solubilized rabbit NADPH–cytochrome P450 reductase (residues 57–679) chromatographed as a 0.93-mer (95.7%) and a 1.81-mer (4.3%), somewhat similar to the behavior seen with the P450 102 flavin domains.

The final set of HPLC size-exclusion chromatography experiments was conducted with the intact P450 102 (residues 1–1048). The purpose of these studies was to determine the character of the equilibrium between 1.5-mer, dimer, trimer, and high molecular weight fraction. To accomplish this, we performed a standard HPLC size-exclusion separation analysis on a preparative quantity of P450 102 and collected fractions, as shown in Figure 5. The preparative quantity of protein used in the primary analysis caused a diminished resolution of the dimer, trimer, and high molecular weight peaks. Three fractions, A, B, and C, were collected, and these corresponded roughly to trimer/high molecular weight peak, dimer/trimer, and 1.5-mer, respectively. Each of the fractions was submitted to reanalysis on the same column and under the same

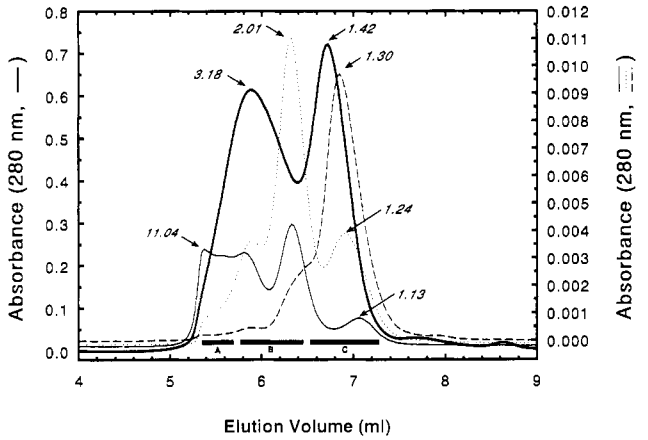

FIGURE 5: Effect of HPLC size-exclusion chromatographic reanalysis on various molecular aggregates of cytochrome P450 102. A preparative quantity of P450 102 (0.237 mg) was submitted to HPLC size-exclusion analysis (thick solid line) in the absence of DTT. Fractions A, B, and C (fraction volumes indicated by boldface horizontal bars near the lower *x*-axis) were collected. A portion of fraction A was reanalyzed to yield (—); upon reanalysis, fraction B yielded (···); and fraction C when reanalyzed gave (- - -). All analyses were under identical conditions, as indicated under Experimental Procedures. The italic numbers within the plot indicate the molecular aggregation state of the respective peak, by reference to molecular weight standards.

chromatographic conditions as before, except that the injected protein concentration was lower. As can be seen from the reanalysis chromatograms, fraction A produced not only trimer and high molecular weight peak, but also dimer and "monomer" peak. Fraction B produced dimer and trimer, but also high molecular weight peak and "monomer". Fraction C yielded "monomer" but also each of the other species. Thus, each fraction reequilibrated to produce some or all of the other molecular aggregate species upon reanalysis. But, surprisingly, each fraction upon reanalysis produced peaks for the "monomer" species that were of smaller apparent aggregation state than that of the 1.42-mer in the primary analysis. That is, fractions A (trimer/high molecular weight peak), B (dimer/trimer), and C (1.42-mer) produced 1.13-mer, 1.24-mer, and 1.30-mer, respectively, and *not* 1.42-mer. The new "monomer" species eluted at volumes distinct from the 1.42-mer; chromatographic repeatability was ≤0.02 mL for each peak from analysis to analysis. In other words, the more disaggregation equilibrations that a fraction experienced, the closer the "monomer" peak eluted to the true monomeric molecular weight. When a similar experiment was performed with DTT-pretreated P450 102 (data not shown), reanalysis of the 1.5-mer peak showed behavior equivalent to the above results, in that the reanalyzed peak eluted at a lower apparent aggregation state.

DISCUSSION

Sedimentation velocity experiments with cytochrome P450 102 in the absence of DTT yielded an $s^0_{20,w}$ (9.244 S) that was similar to the sedimentation coefficients of other proteins having native molecular weights in the vicinity of 200 000. However, the D_{20} varied widely with centrifugal field, radial distance, ionic strength of the medium, and protein concentration. These observations indicated that P450 102 must exist as an aggregating system, in contrast to the expected monomeric character of this soluble cytochrome. Thus, increased pressure due to high centrifugal field or advanced radial position during sedimentation promoted molecular aggregation, as did increased protein concentration or ionic strength. Also, because the dA/dr *vs* r plots remained as a single, comparatively symmetrical peak at all stages of every analysis, relatively rapid equilibration of molecular forms was indicated. The theoretical D_{20} for a spherical dimer (MW 238 838) was calculated as 3.4×10^{-7} cm^2/s; a (minimum) value of 3.1×10^{-7} cm^2/s was measured at low centrifugal field, suggesting that the average sedimenting species was likely to be a dimer.

Initially, we believed that the molecular aggregation of P450 102, as detected by sedimentation velocity, might have been the result of disulfide bond formation between monomers. Consequently, we performed further experiments in the presence of the reducing agent DTT. We found that both $s^0_{20,w}$ (8.507 S) and D_{20} (5.816×10^{-7} cm^2/s) had decreased relative to coefficients measured in the absence of DTT, but were still deviant from the ideal curve in the *s vs D* plot (see Figure 1). The molecular weight estimated for the $s^0_{20,w}$ in the presence of DTT was about 180 000 (approximately a 1.5-mer). The value of D_{20} was still larger than expected, and dA/dr *vs* r plots were still Gaussian during all analyses. Again, this suggested an aggregating system that was in rather rapid equilibrium. Because the apparent molecular weight was not altered significantly and because equilibration between molecular aggregates was still indicated, it appeared doubtful that disulfide reduction was the basis for the DTT effect on P450 102. In agreement with this conclusion, we found in control SDS–PAGE experiments, with and without β-mercaptoethanol (data not shown), that only a very small fraction of the protein was bonded by disulfides.

Friction factor calculations were performed to gain further insight into the aggregation behavior of P450 102 in the absence of DTT. We modeled the f/f_o ratio assuming aggregation states from monomer to octamer, with and without hydration of spherical geometry. The f/f_o and $f/f_{hydration}$ ratios were less than 1 when a monomer molecular weight was assumed, in agreement with our interpretation that P450 102 exists as a molecular aggregate. Of all the other models, only the dimer was physically reasonable, with $f/f_o = 1.50$ and $f/f_{hydration} = 1.32$; these values correspond to axial ratios for a prolate ellipsoid (a/b) of 9.4 and 6.2, respectively. The hydrated case is most biochemically reasonable ($a/b = 6.2$), and suggests that the monomer and/or dimer should deviate significantly from spherical geometry.

Sedimentation equilibrium experiments clarified our interpretation of the native molecular weight of cytochrome P450 102. In the absence of DTT, molecular aggregation was clearly indicated (see Figure 3A), and the data could be fit quite well only to an equilibrium between monomer, dimer, trimer, and tetramer. The computed equilibrium constants indicated that the dimer, trimer, and tetramer would be the predominant forms present. In the presence of DTT, sedimentation equilibrium of P450 102 yielded significantly different results (see Figure 3B). Data readily fit a model indicating the quantitative presence of dimeric enzyme, and the calculated molecular weight (236 000) was in excellent agreement with that known from the covalent structure of holoenzyme. This finding was akin to that determined by sedimentation velocity in the presence or absence of DTT.

HPLC size-exclusion experiments provided further evidence for molecular aggregation in P450 102. Analysis of the purified enzyme showed the presence of >50% aggregated forms. The molecular weights measured for the dimer and trimer corresponded quantitatively to the expected values, thereby suggesting that these species were approximately spherical in geometry. In contrast, no true monomer was

seen. Instead, the lowest molecular weight peak had an apparent aggregation state of 1.45. This molecular form could not have arisen from the dimer, since it would have required a spherical molecule to become significantly more spherical. Thus, the 1.45-mer must be a molecularly-asymmetric form of the monomeric P450 102. This species was present as nearly 50% of the total cytochrome. However, sedimentation studies had suggested that the native enzyme was predominantly dimeric. This disparity may be due to differences in the buffer systems employed (i.e., addition of 0.1 M KCl in HPLC analyses) or differences in hydrodynamic transport (i.e., HPLC was more rapid and also employed a solid matrix). P450 102 has been shown to be sensitive to mechanical forces (Black et al., 1994), and such as exerted by the stationary phase during chromatography could account for the net conversion of some molecular aggregates to monomer. Nonetheless, both approaches indicated asymmetric structure.

Inclusion of DTT in HPLC size-exclusion analyses caused a dramatic shift from aggregated species to the 1.45-mer monomer. However, exhaustive treatment with the reagent failed to produce more than 94% monomer, implying that the equilibrium had been shifted, but not abolished. Thus, the overall conclusion that cytochrome P450 102 monomers exist in equilibrium with at least some dimer, trimer, and tetramer is a consistent finding of all techniques employed in this study. In addition, the effect of DTT clearly is not based on the reduction of adventitious disulfide bonds. The DTT effect, as assessed by HPLC, was extremely slow and required high concentrations of the reagent. Thus, DTT must alter the equilibrium between monomer, dimer, trimer, etc. by binding to one or more of the domains of P450 102 (heme domain, FMN domain, FAD/$NADP^+$ domain). DTT has been shown to bind to the P450 102 heme domain and substrate binding pocket and cause conformational distortion (Ravichandran et al., 1993). The molecular equilibrium may also be shifted toward monomer by reduction of the heme and/or flavins, as evidenced by the effect of dithionite. It is also important to note that the equilibrium can be shifted in the opposite direction as well (toward aggregation) by the addition of reagents such as octyl glucoside. Because the detergent did not promote disaggregation, it is clear that the protein–protein interactions that form dimer, trimer, etc. are not primarily hydrophobic.

Molecular weight analysis of domains of P450 102 showed that the monomeric heme domain was essentially spherical, in agreement with the crystal structure (Ravichandran et al., 1993). While this domain may play a role in regard to the control of aggregate equilibria, it clearly should not contribute to structural asymmetry. On the other hand, the complete flavin domain and the FAD/$NADP^+$ domain both chromatographed as a collection of molecular aggregates, but the structure of the monomer was asymmetric, and aggregation led to progressively more asymmetric molecular forms. Thus, the FAD/$NADP^+$ domain appears to be primarily responsible for both the asymmetry and aggregation of the native P450 102. If our friction factor calculations are correct, the three-domain enzyme should be considerably elongated, with an axial ratio of about 6. Mammalian trypsin-solubilized NADPH–cytochrome P450 reductase is homologous to the P450 102 FMN/FAD/$NADP^+$ domain. The reductase was found to be about 5% dimer, but both the monomer and dimer were symmetrical. Thus, both similarities and differences exist between the *Bacillus* and mammalian reductase domains.

HPLC size-exclusion reanalysis experiments provided two important insights. First, these results proved that each molecular form of P450 102 could reequilibrate to form any of the other forms. This not only provided an additional basis for the *n*-mer equilibrium but also suggested that the rate of equilibration was moderate, perhaps of the same time scale suggested by sedimentation velocity experiments. Second, the monomer produced upon reanalysis exhibited a variety of apparent molecular weights between 1.0-mer and 1.42-mer, with or without DTT present. This showed that the conformation of the P450 102 monomer is dynamic. That is, the monomer can exist in a highly asymmetric form or can fold to assume a more compact, nearly spherical conformation. Some of this effect must be due to reorientation of domains, but it is also likely that intradomain conformation is involved. Thus, the native molecular weight of cytochrome P450 102 might best be described in terms of an equilibrium of conformationally dynamic molecular forms.

Earlier, we noted that the sedimentation velocity behavior of P450 102 was unusual, particularly on the *s vs D* plot. This enzyme and a few others described a curve parallel to that followed by other globular proteins. A curious observation in this connection is that nearly all of these proteins that share the unusual behavior are redox enzymes. Yagi and Ozawa (1962) in their sedimentation studies on the FAD-containing D-amino acid oxidase:benzoate Michaelis complex hypothesized that their results were best explained by changes in the conformation of the protein. An investigation of D-glyceraldehyde-3-phosphate dehydrogenase in the presence of various enzyme "activators" (e.g., KCN) (Elodi, 1958) suggested that the sedimentation properties resulted from dissociation of subunits during activation. The nonredox protein hemagglutinin is a viral protein that has an *a*/*b* ratio for the monomer of about 5.5:1, and aggregates to form more spherical trimers. Sedimentation studies on only cold hemagglutinins (Weber, 1956) showed the unusual *s vs D* behavior. In each of these three cases, molecular aggregation and/or conformational dynamics were apparently at the heart of the peculiar hydrodynamic behavior. Thus, our assertion that cytochrome P450 102 exhibits molecular equilibria and conformational dynamics would appear to be precedented. Such behavior is important in the function of the enzymes discussed above as examples, and, by analogy, it would appear reasonable that such effects will prove to be important in the function of cytochrome P450 102. Our laboratory is actively engaged in the testing of this hypothesis.

ACKNOWLEDGMENT

We thank Dr. Mark A. L. Atkinson for his expert assistance with the analytical ultracentrifuge in the initial stages of this work, and Dr. T. L. Poulos for his kind gift of the P450 102 heme domain used in control experiments.

REFERENCES

Black, S. D. (1992) *FASEB J. 6*, 680–685.
Black, S. D., & Coon, M. J. (1987) *Adv. Enzymol. Relat. Areas Mol. Biol. 60*, 35–87.
Black, S. D., & Martin, S. T. (1994) *FASEB J. 7*, A1167.
Black, S. D., Linger, M. H., Freck, L. C., Kazemi, S., & Galbraith, J. A. (1994) *Arch. Biochem. Biophys. 310*, 126–133.
Boddupalli, S. S., Estabrook, R. W., & Peterson, J. A. (1990) *J. Biol. Chem. 265*, 4233–4239.
Boddupalli, S. S., Pramanik, B. C., Slaughter, C. A., Estabrook, R. W., & Peterson, J. A. (1992) *Arch. Biochem. Biophys. 292*, 20–28.
Conney, A. H. (1967) *Pharmacol. Rev. 19*, 317–366.
Creighton, T. E. (1984) *Proteins: Structure and Molecular Properties*, W. H. Freeman and Company, New York.
Elodi, P. (1958) *Acad. Sci. Hung. 13*, 199–206.

Haugen, D. A., & Coon, M. J. (1976) *J. Biol. Chem. 251*, 7929–7939.
Kim, B. K., & Fulco, A. J. (1983) *Biochem. Biophys. Res. Commun. 116*, 843–850.
Kumosinski, T. F., & Pessen, H. (1985) *Methods Enzymol. 117*, 154–182.
Laemmli, U. K. (1970) *Nature 227*, 680–685.
Laue, T. M., & Rhodes, D. G. (1990) *Methods Enzymol. 182*, 566–587.
Li, H., Darwish, K., & Poulos, T. L. (1991) *J. Biol. Chem. 266*, 11909–11914.
Miles, J. S., Munro, A. W., Rospendowski, B. N., Smith, W. E., McKnight, J., & Thomson, A. J. (1992) *Biochem. J. 288*, 503–509.
Muramatsu, N., & Minton, A. P. (1988) *Anal. Biochem. 168*, 345–351.
Narhi, L. O., & Fulco, A. J. (1986) *J. Biol. Chem. 261*, 7160–7169.
Narhi, L. O., & Fulco, A. J. (1987) *J. Biol. Chem. 262*, 6683–6690.
Nelson, D. R., Kamataki, T., Waxman, D. J., Guengerich, F. P., Estabrook, R. W., Feyereisen, R., Gonzalez, F. J., Coon, M. J., Gunsalus, I. C., Gotoh, O., Okuda, K., & Nebert, D. W. (1993) *DNA Cell Biol. 12*, 1–51.
Oster, T., Boddupalli, S. S., & Peterson, J. A. (1991) *J. Biol. Chem. 266*, 27718–27725.
Ravichandran, K. G., Boddupalli, S. S., Hasemann, C. A., Peterson, J. A., & Deisenhofer, J. (1993) *Science 261*, 731–736.
Ruettinger, R. T., Kim, B.-K., & Fulco, A. J. (1984) *Biochim. Biophys. Acta 801*, 372–380.
Ruettinger, R. T., Wen, L.-P., & Fulco, A. J. (1989) *J. Biol. Chem. 264*, 10987–10995.
Sariaslani, F. S. (1991) *Adv. Appl. Microbiol. 36*, 133–178.
Schenkman, J. B., & Greim, H. (1993) *Handb. Exp. Pharmacol. 105*, 1–739.
Smith, M. H. (1970) in *CRC Handbook of Biochemistry* (Sober, H. A., Ed.) Section C, pp C3–C39, Chemical Rubber Co., Cleveland, OH.
Smith, P. K., Krohn, R. I., Hermanson, G. T., Mallia, A. K., Gartner, F. H., Provenzano, M. D., Fujimoto, E. K., Goeke, N. M., Olson, B. J., & Klenk, D. C. (1985) *Anal. Biochem. 150*, 76–85.
Waterman, M. R., & Johnson, E. F. (1991) *Methods Enzymol. 206*, 1–716.
Waxman, E., Laws, W. R., Laue, T. M., Nemerson, Y., & Ross, J. B. A. (1993) *Biochemistry 32*, 3005–3012.
Weast, R. C. (1988) *CRC Handbook of Chemistry and Physics*, 69th ed., p F-10, CRC Press, Inc., Boca Raton, FL.
Weber, R. (1956) *Vox Sang. 1*, 37–38.
Yagi, K., & Ozawa, T. (1962) *Biochim. Biophys. Acta 62*, 397–401.